

Metal-insulator transitions in tetrahedral semiconductors under lattice change

Shailesh Shukla and Deepak Kumar
School of Physical Sciences, Jawaharlal Nehru University,
New Delhi-110067, India

Nitya Nath Shukla and Rajendra Prasad
Department of Physics, Indian Institute of Technology,
Kanpur-208016, India

April 14, 2024

Abstract

Although most insulators are expected to undergo insulator to metal transition on lattice compression, tetrahedral semiconductors Si, GaAs and InSb can become metallic on compression as well as by expansion. We focus on the transition by expansion which is rather peculiar; in all cases the direct gap at Γ point closes on expansion and thereafter a zero-gap state persists over a wide range of lattice constant. The solids become metallic at an expansion of 13% to 15% when an electron Fermi surface around L-point and a hole Fermi surface at Γ -point develop. We provide an understanding of this behavior in terms of arguments based on symmetry and simple tight-binding considerations. We also report results on the critical behavior of conductivity in the metal phase and the static dielectric constant in the insulating phase and Γ -induced commensurate behaviour. We consider the possibility of excitonic phases and distortions which might intervene between insulating and metallic phases.

1 Introduction

The phenomenon of metal-insulator transition in solids has been a subject of great interest for over five decades and still continues to be a subject of intense research activity [1]. The phenomenon has been observed in a large number of insulators and semiconductors as the lattice is compressed [2, 3]. Thus a basic theoretical model for studying the metal-insulator transition has been the study of electronic properties of a solid whose lattice constant is varied. For odd number of electrons per cell, this is a well-known problem first analyzed by Mott [4]. Here a metal to insulator transition occurs on lattice expansion due to electron-electron interactions. For even number of electrons per cell, at a given lattice constant the solid can be a metal or an insulator depending on the band structure. In this situation the change of lattice constant leads to movement of band edges, which can lead to opening or closing of the energy gap between the valence and conduction bands. Mott [5] pointed out that even for such a transition, the electron-hole correlations play an important role. He argued that a low density of electrons and holes cannot exist, as in this situation the screening is weak and electrons and holes would pair up to form excitons. Over the years the conditions for formation of excitons and possibilities of intervening exciton-condensed phases have been studied by a number of authors [6]–[12]. From these studies a complex scenario for transition from insulator to metal phase emerges under different conditions of band closing.

In this work we theoretically study metal-insulator transition in tetrahedral semiconductors Si, GaAs and InSb under lattice change maintaining the diamond structure. For these solids, the metallic phase occurs both under compression as well as expansion. Here we focus on the transition on expansion, where the metal phase results due to the closing of the hybridization gap. As is well known that at equilibrium lattice constant the s- and p-states mix and give rise to a hybridization gap with four bonding sp states below the gap and four antibonding states above the gap, which results in an insulating state [13]. On expansion, the sp hybridization weakens and the band gap closes resulting in the atomic like ordering of bands which consists of partly filled p-like band at large atomic separations. However, at the band picture level, a new scenario for the transition emerges. The metal phase does not occur immediately following the band closing, but requires a considerable further expansion. The results show that the insulating phase is separated from the metal phase by a substantial range of lattice constant over which the system is an insulator with zero band gap.

In this paper, we present detailed band structure calculations for the above materials. We give simple physical arguments based on symmetry and tight-binding considerations to understand the peculiar existence of the zero-gap insulating phase over a rather wide range of lattice parameter. All the calculations are done within the density functional formalism with local density approximation [14]. Thus the electron-hole correlation effects mentioned above have not been incorporated in the calculation yet.

We also present calculations of some dielectric properties. We have chosen

to examine the behavior of the imaginary part of the zero-wavevector dielectric function, $\epsilon''(\omega)$. On the metallic side

$$\epsilon''(\omega) = \frac{4\sigma(\omega)}{\omega} \quad (1)$$

where $\sigma(\omega)$ denotes the real part of frequency dependent conductivity. On the insulating side, $\epsilon''(\omega)$ behaves at low frequencies (allowing for lifetime to the electronic states) as,

$$\epsilon''(\omega) = A\omega \quad (2)$$

The constant A is seen to be proportional to the static dielectric constant ϵ_s by dispersion relation. Thus on each side of the transition, coefficients of the main ω -dependent term show critical behavior. For a continuous transition one may hope to find some universal relation between these critical behaviors. Accordingly, on the metal side we have calculated the dc conductivity and find its critical behavior as the transition is approached. On the insulating side we have calculated the band gap and the imaginary part of the frequency-dependent dielectric function at zero wavevector. From this we obtain the critical behaviour of the dielectric constant.

The paper is organized as follows. In the next section, we describe the calculational procedure for the various quantities computed here. This is followed by a section containing results and their interpretation. Finally we close the paper with a discussion of the results, some speculations and concluding remarks.

2 Calculational details

For calculating the band structure, we use the full potential linearized augmented plane wave (FP-LAPW) method [15] with the WIEN CODE [16]. The essential features of the calculational procedure are: (i) The unit cell is divided into two parts, atomic spheres and interstitial regions. The basis set is built by functions which are atom-like wavefunctions within atomic spheres, and plane waves in the interstitial regions. The Kohn-Sham orbitals of DFT are now expanded in terms of this basis set. (ii) A modified tetrahedron method is used to do integrations over the Brillouin zone.

These eigenenergies and eigenfunctions are used to calculate the band parameters and response functions mentioned above. On the metallic side, we calculate the dc conductivity, σ_{dc} , using the formula

$$\sigma_{dc} = \frac{e^2}{3} \sum_{n,\mathbf{k}} v_{n,\mathbf{k}}^2 \tau (E_{n,\mathbf{k}} - E_F) \quad (3)$$

where $E_{n,\mathbf{k}}$ is the energy eigenvalue and $\mathbf{v}_{n,\mathbf{k}} = \hbar^{-1} \nabla_{\mathbf{k}} E_{n,\mathbf{k}}$ is the velocity for the eigenstate with quantum numbers n, \mathbf{k} . τ denotes the transport relaxation rate, which is taken to be state-independent here.

On the insulating side, we calculate the energy gap and the imaginary part of the zero-wavevector dielectric constant, $\epsilon''(\omega)$ as function of frequency, ω . For a crystalline solid, the dielectric constant is a matrix of the form $\epsilon_{\mathbf{G}_1 + \mathbf{q}; \mathbf{G}_2 + \mathbf{q}}(\omega)$, where \mathbf{G}_1 and \mathbf{G}_2 are reciprocal lattice vectors. However, here we calculate only the diagonal part corresponding to $\mathbf{G}_1 = \mathbf{G}_2 = \mathbf{q} = \mathbf{0}$, which amounts to neglecting the local effects. The diagonal part is expected to contain the more significant aspects of the critical behavior. For $\omega > 0$, $\epsilon''(\omega)$ is obtained from,

$$\epsilon''(\omega) = \frac{4e^2}{m^2 \omega^2} \sum_{\mathbf{k}; i, f} \langle i; \mathbf{k} | \hat{p}_x | f; \mathbf{k} \rangle \langle f; \mathbf{k} | \hat{p}_x | i; \mathbf{k} \rangle \frac{1}{(E_{f\mathbf{k}} - E_{i\mathbf{k}} - \hbar\omega)^2 + \gamma^2} \quad (4)$$

where \hat{p}_x denotes the x-component of momentum operator, and $f_{n;\mathbf{k}}$ denotes the occupation number of the state $n; \mathbf{k}$. Note that we have allowed for a finite lifetime, γ^{-1} , to the transition between the states [17], which changes the usual δ -function to the Lorentzian. Using dispersion relations, we can obtain in principle, the real part of the dielectric function as well from this calculation. But since our calculations are limited to a small range in frequency, we are able to obtain information only about the static dielectric constant.

3 Results

We first present the results for GaAs. For the sake of simplicity these results do not include the effects of spin-orbit interaction (SO) [18, 19]. Fig.1 shows the band structure plots for four values of the lattice constant, a . Since we are discussing the situation at zero temperature, we take the zero of energy to be the highest occupied level, labelled as E_F . Fig. 1 (a) corresponds to equilibrium lattice constant $a = 10.68 \text{ \AA}$. As a is increased, the direct gap begins to decrease, closing at $a = 10.82 \text{ \AA}$; which is shown in panel (b). The next panel (c) shows the band structure at $a = 11.90 \text{ \AA}$. One notes here that though there is considerable movement of bands, the fermi level E_F remains stuck at Γ_{15} . This situation continues till $a = 12.24 \text{ \AA}$; where the lowest conduction band touches E_F at L as shown in Fig. 1 (d). Thus the system persists as a zero-gap insulator over the lattice constant range from $a = 10.82 \text{ \AA}$ to 12.24 \AA . Thereafter the system becomes metallic with density of states at E_F rising rapidly. In Fig. 2, we show the plots of the density of states (DOS) at 4 corresponding values of the lattice parameter. In Fig. 2 (b) and (c) the DOS around E_F is nonzero but too small to be seen in the figures. These plots further confirm the zero band gap state persisting in the entire region from $a = 10.82 \text{ \AA}$ to 12.24 \AA .

Fig. 3 shows band structure results for Si for four values of lattice constant. Fig. 3 (a) shows the results for the equilibrium lattice constant $a = 10.26 \text{ \AA}$. Here the smallest band gap is between the valence band at Γ and the conduction band around X in $-X$ direction. In Fig. 3 (b) at $a = 11.17 \text{ \AA}$; one sees that the direct gap at Γ becomes the smallest. With further expansion at $a = 11.39 \text{ \AA}$; the direct gap closes as seen in Fig. 3 (c). Thereafter the system stays in the

zero gap state till $a = 11.96 \text{ \AA}$, where the conduction band at L touches E_F as seen in Fig. 3(d). The density of states for Si on lattice expansion shows behavior similar to that of GaAs and hence is not shown here. The calculation confirms that the zero gap condition occurs over the range $a = 11.39 \text{ \AA}$ to 11.96 \AA in this case.

We now provide some arguments that enable us to understand this peculiar behavior in terms of the symmetry of the structure and the symmetry of the atomic orbitals involved in the formation of the relevant bands. We present these arguments in terms of tight-binding (TB) considerations [13, 20]. For GaAs, the unit cell has two atoms per cell to be denoted as c and a, each with a tetrahedral surrounding of the unlike atoms. For Si, the two atoms are identical but are taken to belong to different sublattices c and a. For a reasonable description of the band structure of these solids we require a minimum of eight orbitals, one s- and three p-orbitals of each c and a atoms. These are labeled as: $s^c; s^a; p_x^c; p_y^c; p_z^c; p_x^a; p_y^a; p_z^a$. For details we refer to the book by Harrison [13].

Using the TB method we can easily understand the degeneracies of the eight bands at symmetry points like Γ, X, W and in symmetry directions like $\Gamma-X$ etc., as due to symmetry the tight-binding Hamiltonian matrix [13] is simplified and is reducible. At Γ point, we have two s-type levels ϵ_1 and two p-type levels ϵ_{15} each with a degeneracy of three. These eight levels along with their degeneracies denoted by D, are given by [13]

$$E_s^{1;2}(\Gamma_1) = \frac{\epsilon_s^c + \epsilon_s^a}{2} + \frac{\hbar^2}{2} \left(\frac{\epsilon_s^c - \epsilon_s^a}{2} \right)^2 + 16M_{ss}^2 \frac{i_1}{2} D = 1 \quad (5)$$

$$E_p^{1;2}(\Gamma_{15}) = \frac{\epsilon_p^c + \epsilon_p^a}{2} + \frac{\hbar^2}{2} \left(\frac{\epsilon_p^c - \epsilon_p^a}{2} \right)^2 + 16M_{xx}^2 \frac{i_1}{2} D = 3 \quad (6)$$

At X point, we have four hybridized sp_x levels and two p-type levels of degeneracy two each corresponding to orbitals p_y and p_z , given by

$$E_{sp}^{1;2} = \frac{\epsilon_s^c + \epsilon_p^a}{2} + \frac{\hbar^2}{2} \left(\frac{\epsilon_s^a - \epsilon_p^c}{2} \right)^2 + 16M_{sp}^2 \frac{i_1}{2} D = 1 \quad (7)$$

$$E_{sp}^{3;4} = \frac{\epsilon_s^a + \epsilon_p^c}{2} + \frac{\hbar^2}{2} \left(\frac{\epsilon_p^c - \epsilon_s^a}{2} \right)^2 + 16M_{sp}^2 \frac{i_1}{2} D = 1 \quad (8)$$

$$E_p^{1;2} = \frac{\epsilon_p^c + \epsilon_p^a}{2} + \frac{\hbar^2}{2} \left(\frac{\epsilon_p^c - \epsilon_p^a}{2} \right)^2 + 16M_{xy}^2 \frac{i_1}{2} D = 2 \quad (9)$$

where $\epsilon_{sp}^{c;a}$ denote the energies of the four atomic levels involved, and M's denote the combinations of matrix elements between orbitals on the neighboring atoms. The TB parameters ϵ_s^c etc. are taken from Ref.[13]. Qualitatively the band structures of GaAs and Si obtained by using TB method are similar to that shown in Figs. 1 and 3 respectively and therefore are not shown here.

For Si, the four sp -levels become a set of two degenerate levels at X point. Along the $\Gamma-X$ line, we have a set of four sp_x hybridized levels made up from orbitals $s^c; s^a; p_x^c$ and p_x^a , which have been labelled sp_1, sp_2, sp_3 and sp_4 . The other four orbitals $p_y^c; p_z^c; p_y^a; p_z^a$ form a set of two doubly degenerate levels labelled as p_a and p_b . A very similar structure exists for L point and on the

L line. Here again the two s-orbitals hybridize with two linear combinations of p-orbitals (the combination which points along the cube diagonal for each a and c atom s) to give rise to a set of four sp-hybridized levels. The remaining four p-orbitals with combinations that point in the two perpendicular directions to the cube diagonal, then split into a set of two doubly degenerate levels. Since these features of the bands are a result of basic lattice symmetry, this degeneracy structure is seen in the full calculation shown in Figs. 1 and 3. Further note that the bands sp_1 and sp_3 have an upward curvature, while the bands sp_2 and sp_4 have downward curvature with k . Similarly the bands p_b and p_a curve downwards and upwards respectively.

We can now discuss the relative positioning of these eight bands as the lattice constant is changed. It suffices to consider the ordering of levels along the symmetry directions Γ , X and L and at the symmetry points Γ , X and L. At the equilibrium lattice constant, two bonding sp-hybridized bands sp_1 and sp_2 and doubly degenerate bonding p-band p_b are below E_F and the remaining antibonding bands sp_3 and sp_4 , and the degenerate band p_a are above E_F . At Γ , sp_2 and sp_4 bands become degenerate respectively to p_b and p_a bands giving rise to two three fold degenerate levels Γ_{15} . For GaAs, the band gap at Γ is between triply degenerate Γ_{15} level and a sp_3 -level Γ_1 . For Si at equilibrium the band gap is indirect between p_b and sp_4 bands, but after a stretching up to 11.17 a.u.: the same ordering as in GaAs happens at Γ as seen in Fig. 3(b). For subsequent expansion both the solids show same band movements.

As the lattice is expanded, Γ_1 and Γ_{15} levels approach each other and at some point they touch leading to a zero gap situation at Γ where one now has a four-fold degeneracy. On further expansion, the band sp_2 shifts downwards, while the sp_3 band sticks to Γ_{15} to maintain the degeneracy to three. Since sp_2 band and p_b bands curve downwards, while sp_3 curves upwards, four full bands stay below E_F and the four full bands above. For some range of lattice expansion this situation persists as the sp_3 band remains above Γ_{15} . Thus the system stays in the zero-gap insulating state. During this range of lattice expansion sp_3 band shows little movement around Γ but sp_2 band moves down considerably. Note the ordering of bands at X has changed; both Γ_1 levels are below E_F now. In this situation the bands have assumed the ordering that one would expect from atomic picture, i.e. the two s-like bands below the two p-like bands. The metallic state is reached on further expansion when the sp_3 band bends downwards along Γ line to cross E_F . At this point an electron like fermi surface near L and a hole like fermi surface around Γ begin to build up leading to a rapid increase in density of states at E_F . Note that the zero-gap state results because the degeneracy at Γ_{15} levels has to be maintained at 3 due to the symmetry.

We next give the results for InSb, whose optical gap is rather small (0.23 eV). One therefore expects this peculiar behaviour to occur at smaller expansions which are experimentally feasible. Its band structure at the equilibrium lattice constant 12.24 a.u. is shown in Fig. 4(a). As in Reference 22, we also find it to have a vanishing gap at the Γ point. Including spin-orbit coupling also does not lead to a gap [23]. However, the expansion leads to similar zero gap state

which persists upto $a = 13.85 \text{ \AA}$. This is shown in Fig. 4(b). Again the metal phase occurs when the conduction band dips to fermi level at the L point, where the gap in equilibrium was 1.4 eV. Curiously in Si and GaAs also, the gap at L point has approximately the same value when the gap at Γ point closes. In spite of the small direct band gap in InSb, the metallization occurs at about 13% expansion and in this respect it is no different from Si or GaAs. It is interesting to note that in Si the zero gap state persists for only 4% expansion but in GaAs as well as in InSb, it lasts over 13% expansion. This can be attributed to the nature of bonding of these solids; bonding in Si is purely covalent, while in GaAs and InSb it has some ionic character [24, 25].

We have also calculated the band gaps for both GaAs and Si at lattice parameter values close to $a_I = 10.82 \text{ \AA}$ and 11.39 \AA respectively at which their direct gaps vanish. Its plot with $t = \frac{a_I - a}{a_I}$ (Fig. 5) shows that the gap variation with lattice parameter is approximately linear in this region.

Next we present the calculation of some dielectric properties. Figs. 6(a) and 6(b) show plots of $\epsilon''(\omega)$ with ω for a number of values of a close to the transition in GaAs and Si respectively. One can see that these plots are linear in the small frequency range ($\omega \rightarrow 0$) with the slopes rising as the transition is approached. In Fig. 7 we present a plot of the slope A of curves in Fig. 6(a), which is proportional to static dielectric constant ϵ_s , with t . The static dielectric constant is seen to exhibit power law with t and diverges as $t \rightarrow 0$.

$$\epsilon_s \propto t^{-1} \quad (10)$$

The exponent is found to be 1.8 ± 0.05 for both Si and GaAs.

On the metal side we have calculated the static conductivity σ_{dc} around the transition point and have plotted it with t in Fig. 8(a) and 8(b). This data can again be fitted to a power law in t , where now $t = \frac{a - a_M}{a_M}$ and a_M denotes the lattice constant at which the system becomes a metal.

$$\sigma_{dc} \propto t^b \quad (11)$$

The values of the exponent are $b = 2.01 \pm 0.09$ for GaAs and 1.80 ± 0.05 for Si. On the basis of this calculation we cannot claim them to be equal, but the calculations are quite limited by numerical accuracy in the regime of small conductivities as counting of small density of states in the Brillouin zone is prone to errors. Interestingly these exponents are equal within numerical accuracy to the values obtained for these exponents for CsI, which undergoes a continuous metal-insulator transition on lattice compression [26].

4 Discussion

It is clear from the above analysis that the insulator metal transition and associated peculiar behaviour on lattice expansion results from the features of band structure at points Γ , X and L which are basically governed by the symmetry of the underlying lattice and the symmetry of s and p orbitals. We expect all

sp bonded tetrahedral semiconductors to show this behaviour. Further we emphasize that the transition will occur irrespective of the exchange-correlation potential used, as it is symmetry driven, apart from slight differences in the values of transition point lattice parameters a_T and a_M [21, 27]. The zero gap state over an extended range of lattice constants is admittedly somewhat hypothetical, as it is based on the assumption that the diamond structure is maintained on expansion. With the weakening of the hybridization, it is not clear if the tetrahedral symmetry would be the preferred one. However, these peculiar band effects may underlie interesting physics arising from electron-electron interaction and electron-lattice interaction. We discuss some of these issues below.

An important issue is the role of electron-hole interactions as mentioned in the introduction, which may lead to a new exciton-condensed ground states in systems with small or zero band gaps [10]. We first discuss the situation from the insulating side, where Knox [6] argued, that when the binding energy, E_b , of the exciton becomes larger than the energy gap, E_g , there would be a spontaneous formation of excitons. The binding energy of the exciton is given by, $E_b = \epsilon_s^2$ units of Rydbergs, where ϵ_s denotes the reduced mass of the electron hole pair in units of electron mass. When the energy gap is an indirect one, ϵ_s remains finite as the gap closes and the E_b can become larger than E_g resulting in an exciton-condensed phase which is a charge or spin density wave [7]–[10]. However, in the present case the concerned gap is a direct one, which also leads to the divergence of ϵ_s due to different symmetry of the bands across the gap at the Γ point. Thus E_g and E_b both tend to zero as the gap closes. If one assumes ϵ_s / E_g , it is seen that the spontaneous formation of excitons can occur only if $\epsilon_s / E_g < 0.5$.

In the calculations described above, we have obtained the variations of both ϵ_s and E_g with reduced lattice parameter, t . This yields $\epsilon_s / E_g \approx 1.8$ for both Si and GaAs. Thus the exciton phase does not occur in these materials according to Knox criterion. The possibility of the existence of the exciton instability for the direct gap case has been examined further by going beyond RPA [28]–[29]. Inclusion of Hartree Fock corrections [28] or the contribution of excitons themselves [29] to polarizability does not alter the result that the exciton instability does not occur in this situation.

Though the Knox criterion for the occurrence exciton-condensed state is not satisfied here, we believe that the stability of the zero gap state needs to be examined further, as due to its high polarizability it would be susceptible to other instabilities. Distortions of the Jahn-Teller type that lift the degeneracy of the touching bands at Γ point are possible, but their precise nature would depend upon the electron-phonon interaction. The instability towards distortion is quite evident if we examine the situation from metallic side. Here the electron and hole Fermi surfaces are separated by a vector $\mathbf{Q} = \frac{2\pi}{a}(1;1;1)$. Under conditions of proper nesting this state could be unstable to a distorted metal state with wavevector \mathbf{Q} . This matter is under further investigation.

We conclude by remarking that the band structure calculations on tetrahedral semiconductors reported here are indicative of an unusual insulator to metal transition in which there is an intermediate zero-gap state over a consid-

erable stretch of lattice parameter. Several factors like stability of symmetry with expansion, electron-electron interactions and electron phonon interactions would modify the picture given by these calculations. We feel that there is a good possibility of observing some of these peculiar features, particularly the ones associated with the zero-gap state in InSb. Finally we also obtain some common dielectric behaviour in this class of solids.

It is a pleasure to thank Profs. S.C. Agarwal, M.K. Harbola and R.C. Budhani for helpful discussions. This work was supported by the Department of Science and Technology, New Delhi under project Nos. SP/S2/M-46/96. and SP/S2/M-51/96.

References

- [1] For a review see, for example, M. Imada, A. Fujimori, Y. Tokura, *Rev. Mod. Phys.* 70, 1039 (1998).
- [2] J. Zhao and J. P. Lu, *Phys. Rev. B* 66, 092101 (2002).
- [3] G. J. Ackland, *Rep. Prog. Phys.* 64, 483 (2001).
- [4] N. F. Mott, *Proc. Roy. Soc. Lond.* 62, 416 (1949).
- [5] N. F. Mott, *Phil. Mag.* 6, 287 (1961).
- [6] R. S. Knox, *Solid State Physics, Supplement 5*, Ed. F. Seitz, D. Turnbull and H. Ehrenreich (Academic Press, New York, 1963), 100.
- [7] J. des Cloizeaux, *J. Phys. Chem. Solids* 26, 259 (1965).
- [8] L. V. Keldysh and Yu. V. Kopaev, *Fiz. Tverd. Tela* 6, 2791 (1965) (*Soviet Phys.- Solid State* 6, 2219 (1965)).
- [9] W. Kohn, *Phys. Rev. Lett.* 19, 439 (1967).
- [10] B. I. Halperin and T. M. Rice, *Rev. Mod. Phys.* 40, 755 (1968); in *Solid State Physics, Vol. 21*, Ed. F. Seitz, D. Turnbull and H. Ehrenreich (Academic Press, New York, 1968).
- [11] J. Zittartz, *Phys. Rev.* 164, 575 (1967).
- [12] N. F. Mott and E. A. Davies, *Phil. Mag.* 17, 1269 (1965).
- [13] W. A. Harrison, *Electronic Structure and the Properties of Solids* (W. H. Freeman, San Francisco, 1980), p. 61.
- [14] For a review, see, for example, W. Kohn and P. Vashishta in *Theory of the Inhomogeneous Electron Gas*, Ed. S. Lundqvist and N. H. March (Plenum Press, New York, 1983).
- [15] D. Singh, *Plane Waves, Pseudopotentials and LAPW method* (Kluwer Academic, Boston, 1994).
- [16] P. Blaha, K. Schwarz, and J. Luitz, *WIEN 97, A Full Potential Linearized Augmented Plane Wave Package for Calculating Crystal Properties* (Karlheinz Schwarz, Vienna, 1999).
- [17] We have broadened the energy levels by 0.1 eV.
- [18] The spin-orbit (SO) band structure for GaS calculated by us at equilibrium lattice constant agrees well with the results reported in literature [19] and on expansion shows the same trend as shown in Fig. 1. (see Fig. 4) The lattice constants at which the band gap vanishes and at which the system becomes metallic are approximately same as calculated without including SO.

- [19] M . P . Surh, M . F . Li and S . G . Louie, Phys. Rev. B 43, 4286 (1991); G . B . Bachelet and N . E . Christensen, Phys. Rev. B 31, 879 (1985).
- [20] D . J . Chadi and M . L . Cohen, Phys. Stat. Solidi (b) 68, 405 (1975).
- [21] Ref.[27] has shown that the LDA gives correct volumes at which metallization occurs as a function of pressure.
- [22] A . Svane and E . Antoncik, J Phys. C 20, 2683 (1987).
- [23] M . Cardona, N E Christensen, and G Fasol, Phys. Rev. B 38, 1806 (1988).
- [24] H . Fujita, K . Yamachi, A . Akasaka, H . Irie and S . Masunaga, Journal of the Physical Society Japan 68, 1994 (1999).
- [25] Eugene J . Mele and J . D . Joannopoulos, Phys. Rev. B 24, 3145 (1981).
- [26] S . Shukla, D . Kumar, N . N . Shukla and R . Prasad, to be published.
- [27] S . Wei and H . Krakauer, Phys. Rev. Lett. 55, 1200 (1985).
- [28] J . K . Kubler, Phys. Rev. 183, 703 (1969).
- [29] L . J . Sham and T . V . Ramakrishnan in The Physics of Semimetals and Narrow Gap Semiconductors edited by D . L . Carter and R . T . Bate (Pergamon Press, New York, 1971) p . 209.

FIGURE CAPTIONS

Fig. 1. Band structure of GaAs along some symmetry directions at different lattice constants as indicated in the figure. Panel (a) corresponds to the equilibrium lattice constant. Along $\Gamma-X$ direction, labels sp_1 , sp_2 , sp_3 and sp_4 denote the sp hybridized bands and p_a , p_b , the doubly degenerate p bands. Degeneracies of the bands are denoted by numbers 1 and 2.

Fig. 2. Density of states for GaAs at different lattice constants as indicated in the figure.

Fig. 3. Same as Fig. 1 but for Si.

Fig. 4. Band structure of InSb at lattice constants corresponding to (a) equilibrium (b) when metallisation begins.

Fig. 5. Band gap variation in GaAs and Si as a function of $t = \frac{a_t - a}{a_t}$. The dashed lines show t by $t^{1.03}$ and $t^{1.08}$ respectively.

Fig. 6. (a) Imaginary part of dielectric function of GaAs versus frequency for various lattice parameters between lattice constant 10.78 a.u (top curve) and 10.74 a.u (last curve at the bottom). (b) Same as (a) but for Si between lattice constant 11.37 a.u (top curve) and 11.33 a.u (last curve at the bottom).

Fig. 7. Slope of the curves shown in Fig. 6(a) in region $!! > 0$ as a function of $t = \frac{a_t - a}{a_t}$. The dashed line shows power law t by $t^{1.79}$.

Fig. 8. (a) Plot of d.c conductivity as a function of $t = \frac{a - a_M}{a_M}$ for GaAs. The dashed line shows power law t by $t^{2.01}$. (b) Same as (a) but for Si. The dashed line shows power law t by $t^{1.80}$.

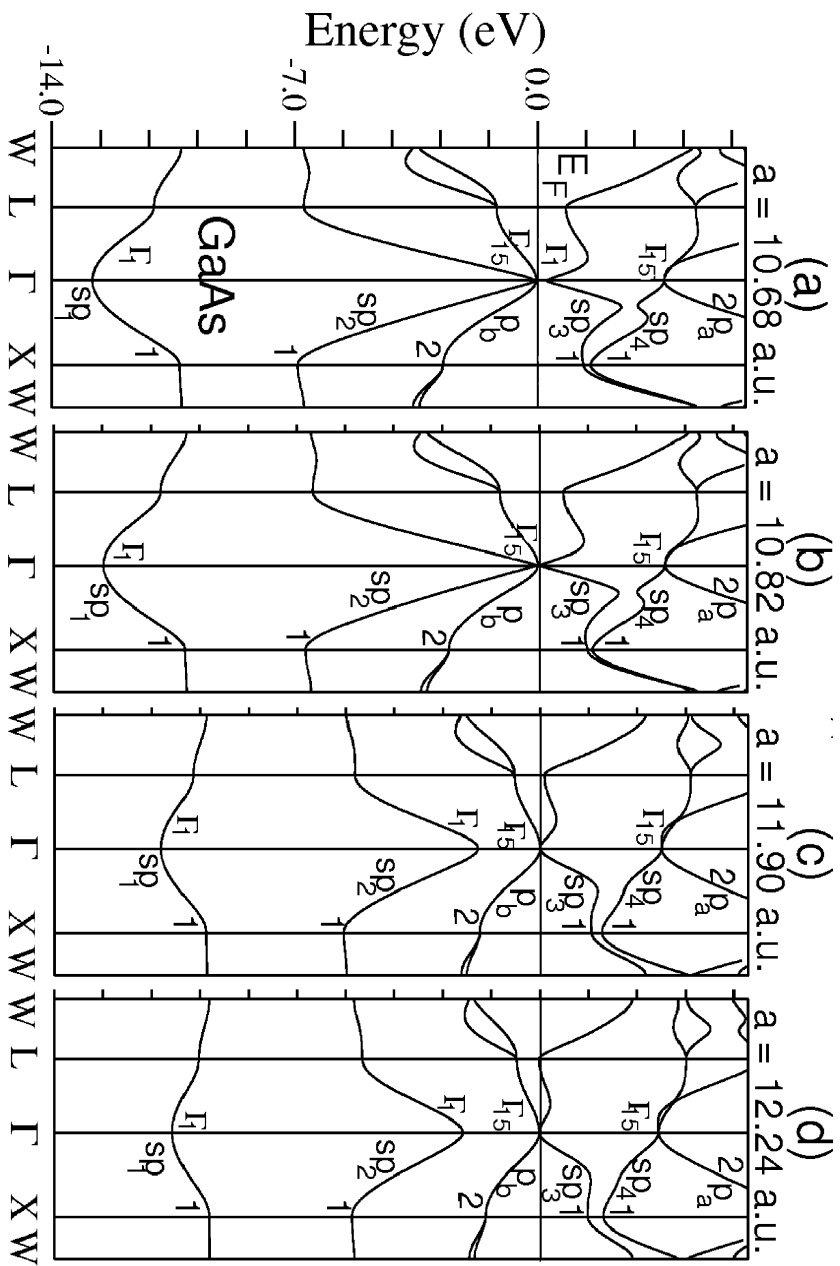


Fig.1

Metal-insulator transitions in tetrahedral semiconductors under lattice change
 Shailesh Shukla, Deepak Kumar, Nitya Nath Shukla and Rajendra Prasad

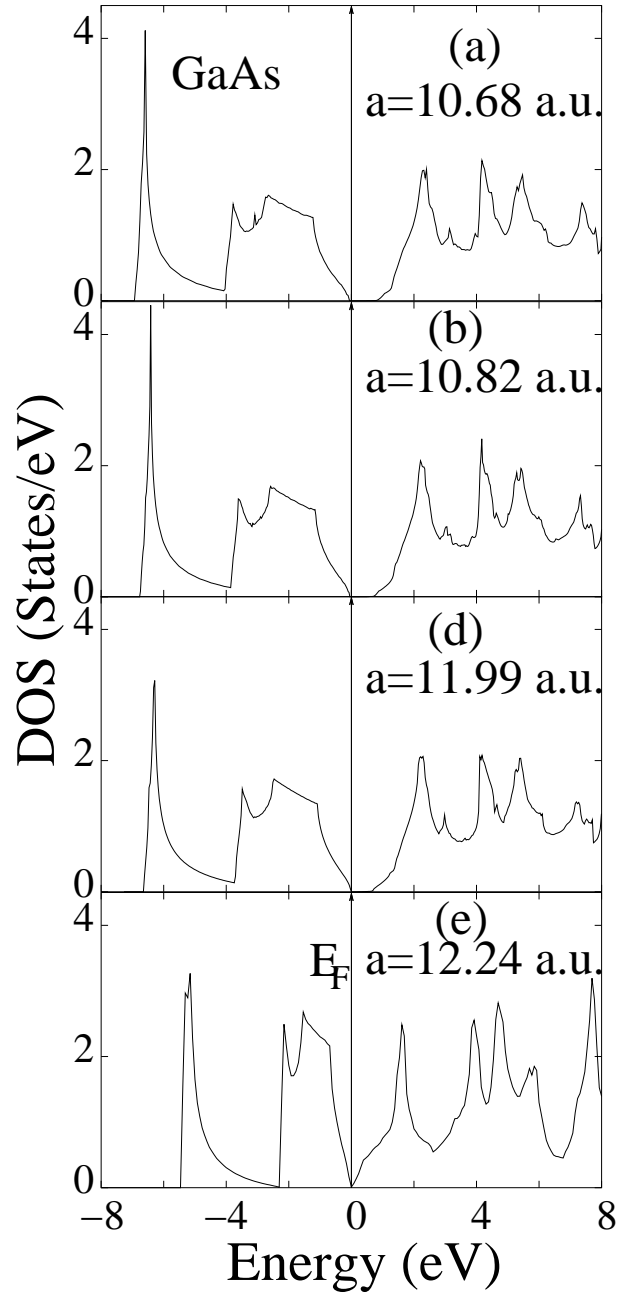


Fig.2

Metal–insulator transitions in tetrahedral semiconductors under lattice change

Shailesh Shukla, Deepak Kumar, Nitya Nath Shukla and Rajendra Prasad

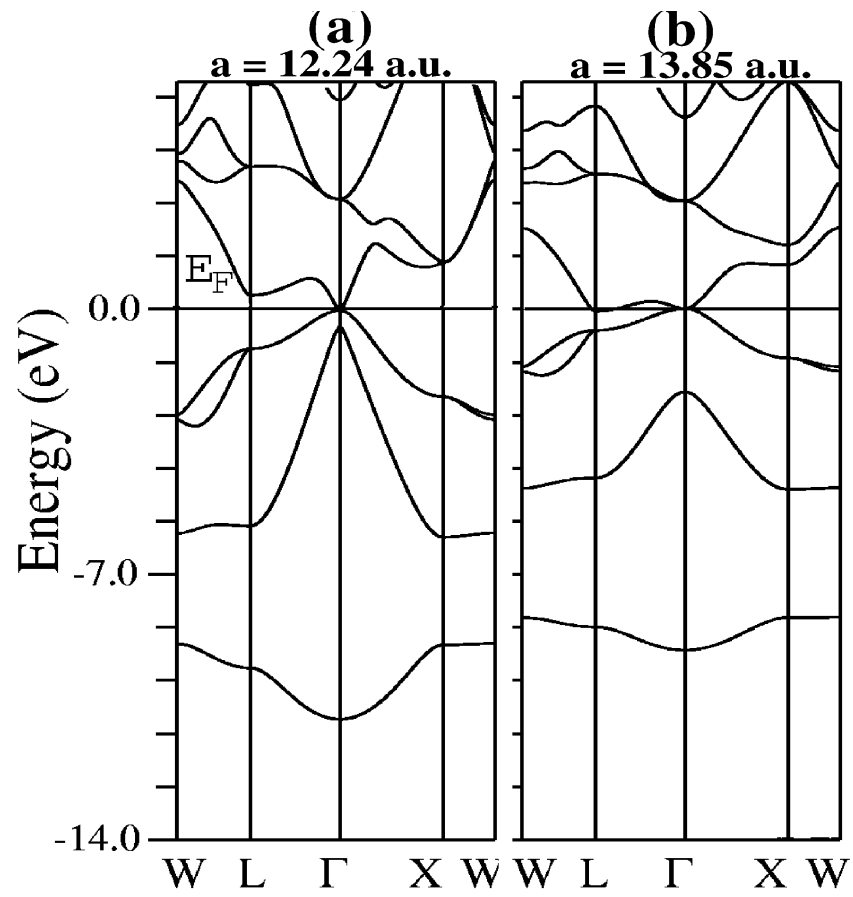


Fig.4

Metal-insulator transitions in tetrahedral semiconductors under lattice change
 Shailesh Shukla, Deepak Kumar, Nitya Nath Shukla and Rajendra Prasad

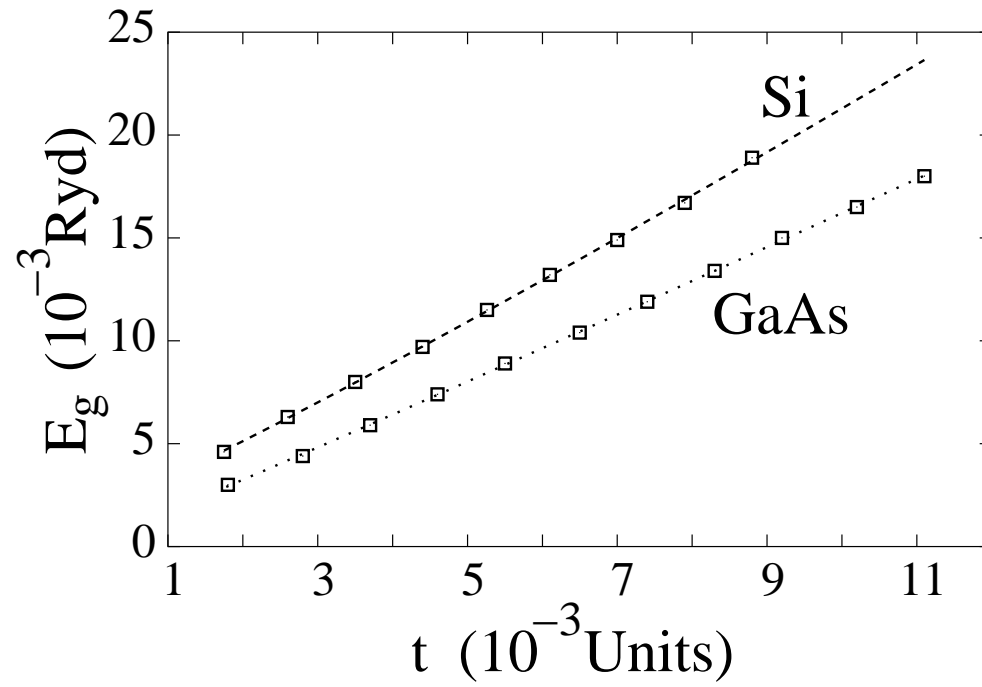


Fig. 5

Metal–insulator transitions in tetrahedral semiconductors under lattice change

Shailesh Shukla, Deepak Kumar, Nitya Nath Shukla and Rajendra Prasad

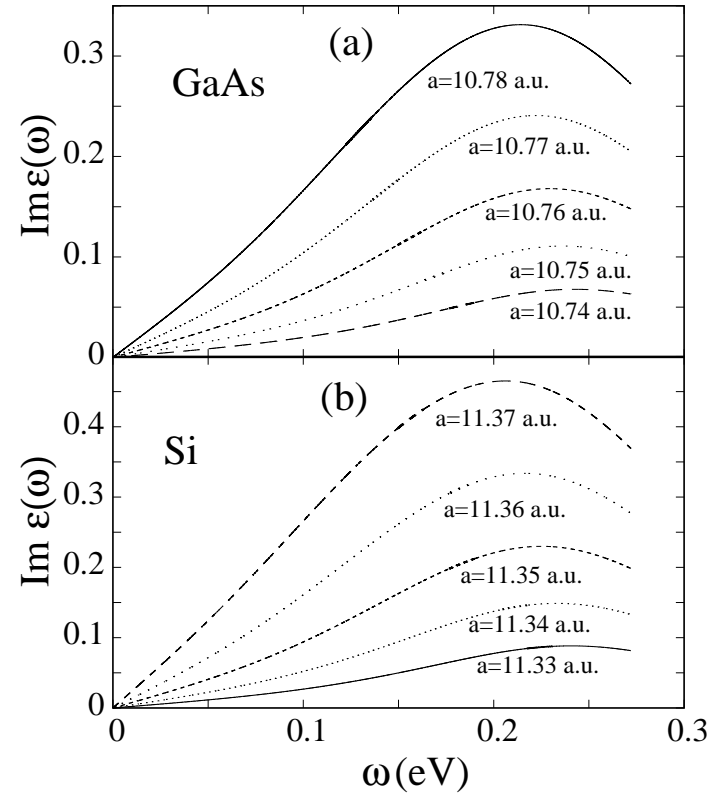


Fig. 6

Metal–insulator transitions in tetrahedral semiconductors under lattice change
 Shailesh Shukla, Deepak Kumar, Nitya Nath Shukla and Rajendra Prasad

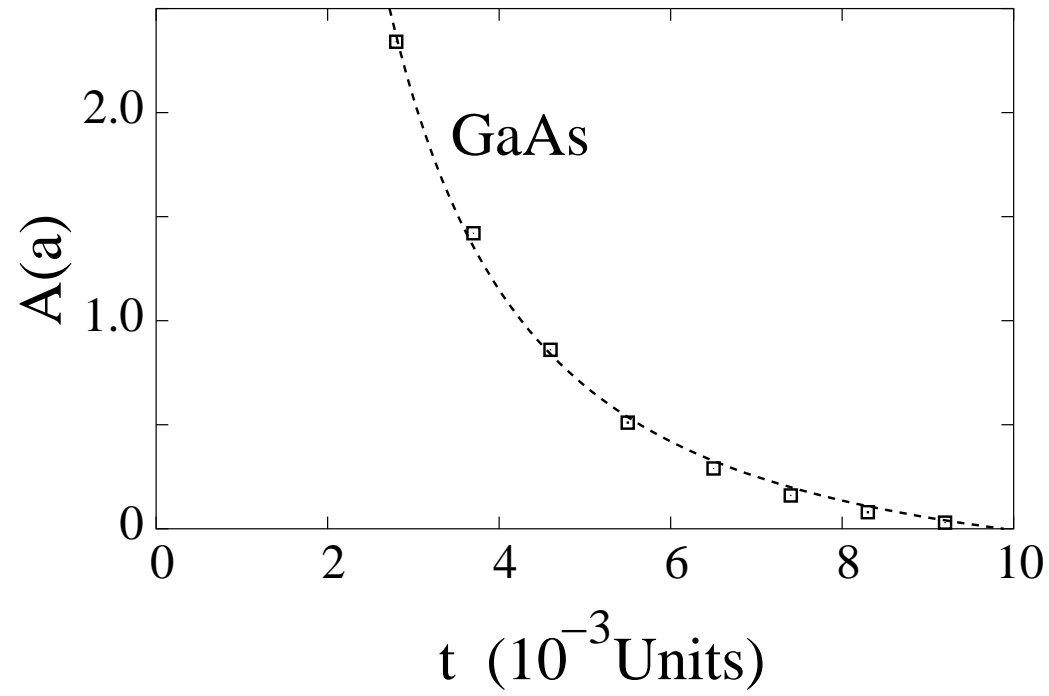


Fig. 7

Metal–insulator transitions in tetrahedral semiconductors under lattice change

Shailesh Shukla, Deepak Kumar, Nitya Nath Shukla and Rajendra Prasad

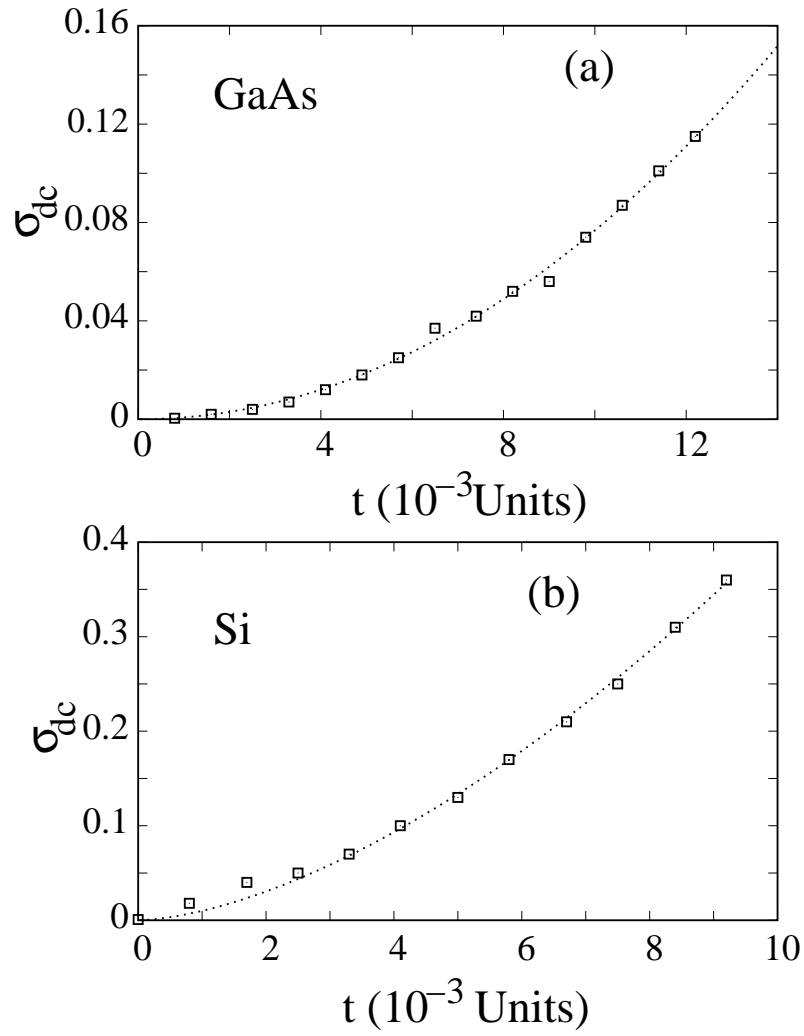


Fig. 8

Metal–insulator transitions in tetrahedral semiconductors under lattice change
 Shailesh Shukla, Deepak Kumar, Nitya Nath Shukla and Rajendra Prasad